BLADE DESIGN AND TIP CLEARANCE FLOW ANALYSIS FOR A COMPACT HIGH-PRESSURE COMPRESSOR REAR STAGE

C. Köhler - C. Helcig - V. Gümmer

Chair of Turbomachinery and Flight Propulsion
Technical University of Munich
Boltzmannstraße 15
85748 Garching
Deutschland

ABSTRACT

One way to mitigate the environmental impact of an aero-engine is the increase of thermal efficiency by implementing higher core engine pressure ratios. A higher core engine pressure ratio inevitably leads to a reduction of the compressor's cross-sectional area and thus to an increase of the relative rotor tip clearance heights. The large clearances cause detrimental aerodynamic effects, which penalize the compressor's operational behavior. This paper presents the numerical design efforts for a compact high-pressure compressor rear stage as well as measures to mitigate the detrimental effects resulting from high rotor tip clearances. To reduce turnaround times, an iterative adaption, including 3D features of the rotor and stator, is carried out by steady single blade row calculations on coarse meshes. It appears that the designed compressor blading shows a stall initiation at the rotor tip due to the strong tip leakage flow. A conducted tip clearance sensitivity study substantiates this. As the relative rotor tip clearance is reduced, the stall margin as well as the design point efficiency of the stage increase. Finally, a novel way of analyzing the stability of a tip-critical rotor blade row is presented by analyzing the circumferentially averaged entropy distribution within the rotor tip clearance.

KEYWORDS

COMPACT, HIGH-PRESSURE, COMPRESSOR DESIGN, NUMERICS, TIP-CRITICAL, STALL, TIP STALL, ENTROPY, LOSSES

NOMENCLATURE

Latin symbols

cl	Relative rotor clearance height, [%]
i	Incidence, [°]
k	Turbulence Kinetic Energy, [m^2/s^2]
p, p_t	Static pressure, total pressure, [Pa]
T_t	Total temperature, [K]
SM	Stall margin, [-]
$y+$	Dimensionless wall distance, [-]

Greek symbols

α	Flow angle in abs. frame, [°]
η_{pol}	Polytropic efficiency, [-]
ω	Turbulence Eddy Frequency, [1/s]

Acronyms

BC	Boundary Condition
CFD	Computational Fluid Dynamics
DP	Design Point
GC	Geometrical Center
HPC	High-Pressure Compressor
LES	Large Eddy Simulation
OPR	Overall Pressure Ratio
PIV	Particle Image Velocimetry
TPR	Total Pressure Ratio
SBR	Single Blade Row

INTRODUCTION

The continuous growth of the air transport sector provides both benefits and challenges for the aviation industry. Even in the most pessimistic scenario, the number of annual passengers is expected to grow to 5.8 billion by the year 2035. It will further increase the impact of aviation on the environment, thus, leading to high demand for more environmentally friendly and more economical aircraft engines (International Air Transport Association, 2016). Together with the future standards and goals set by the aeronautical community, this requires aero-engine manufacturers to realize more advanced and eco-friendly aero-engines with increased thermal efficiency. High thermal efficiency can be achieved by implementing a high overall pressure ratio (OPR) for the engine's compressor. However, a further increase in core engine pressure ratio leads to an inevitable reduction of the core engine size, cross-sectional area and blade height. The decrease in blade height leads to large relative rotor tip clearance heights. These large relative clearances result from the limitation of the tip gaps on an absolute scale to avoid rubs and due to fixed manufacturing tolerances. The resulting geometrical changes introduce new high-pressure compressor (HPC) design challenges, as detrimental aerodynamic effects substantiate. The effects include pronounced secondary flow phenomena, stronger blade tip vortices, and an increased boundary layer growth in the end wall regions. These flow phenomena penalize the compressor's operational behavior (stall margin) and aerodynamic performance (efficiency). The impact of large rotor tip clearance and the associated flow phenomena were investigated thoroughly by numerous researchers. Copenhaver et al. (1996), did numerical as well as experimental investigations of different tip clearance heights for a transonic fan. They observed a significant decrease of rotor efficiency as well as stall margin as the relative rotor tip clearance was increased. Further experimental and numerical investigations for different tip clearance heights were performed by Yamada et al. (2013). Their studies on a low-speed axial compressor showed a vortex-breakdown within the rotor tip leakage flow as near-stall operating conditions were considered. This breakdown could be associated with the formation of large blockage regions at the outer casing. A similar vortex breakdown characteristic was presented by Inoue et al. (2004). They performed an experimental study for a low-speed axial compressor at different rotor tip clearance heights. Hah et al. (2014) compared particle image velocimetry (PIV) measurements and large eddy simulation (LES) results for a research compressor at different rotor tip clearance heights. They found that strong pressure fluctuations near the rotor leading edge occur and an instability vortex forms near the leading edge for the large tip gap case at near stall operation. Hah et al. (2015) further analyzed different rotor tip clearance heights by comparing PIV and LES results. It was found that the fundamental structure of the rotor tip clearance flow changes as the clearance height is increased. One flow effect associated with large rotor tip clearances is the appearance of double leakage flow as described by Hah (2017). By again utilizing numerical LES as well as PIV analyses, Hah (2017) found that the double leakage flow causes a breakdown of the rotor's tip vortex. At near stall conditions, this breakup appears close to the rotor leading edge. Furthermore, Erler et al. (2016) concluded that both the double leakage as well as the meridional momentum of the flow near the rotor tip determine the penalty in stall margin and efficiency for a tip-critical compressor stage. Mitigation of the double leakage and increase of the meridional momentum lead to an enhancement of their presented compressor design. Another flow phenomenon associated with the initiation of stall near the rotor tip is the stall initiation through a spike stall. Within the investigations of Vo et al. (2008), a criterion for spike stall initiation was established. They identified two criteria, which mark the onset of the spike stall. For one part, stall initiates when the interface between the oncoming main flow and the tip clearance flow aligns with the leading edge plane at the rotor tip. Apart from that, an upstream propagation of the trailing edge flow around a neighboring rotor tailing edge back into the blade passage must occur. This phenomenon is referred to as trailing edge backflow.

The numerical investigations presented within this paper divide into three parts. First, we present an iterative design scheme for designing a compressor with a large rotor tip clearance. To speed up the design process while capturing the crucial three-dimensional flow features, an approach as proposed

Table 1: **Numerical setup of full stage and single blade row simulations**

	Full Stage (Fine Meshes)	**SBR (Coarse Meshes)**
No. of Mesh Elements	$1.0 \cdot 10^6$ - $2.2 \cdot 10^6$	$1.1 \cdot 10^5$ - $2.5 \cdot 10^5$
No. of Rotor Tip Gap Elements	45	11
y+ at End Walls	$\mathcal{O}(1)$	$\mathcal{O}(10)$
Fluid Model	Air Ideal Gas (Compressible)	
Turbulence Model	low-Re k-ω	
Inlet BC Definition	p_t-, T_t, α, k and ω-Distribution	
Outlet BC Definition	Scalar Mass Flow, p-Shape	
Pitch-Wise BC Definition	Periodic Boundary Conditions	
Blade Row Connection	Mixing Planes (fixed p_t)	Not Applicable

by Denton (2017) is used. This approach utilizes three-dimensional CFD investigations throughout the design by combining coarse mesh and fine mesh simulations. Second, a clearance sensitivity study is carried out with the final redesign of the compressor to determine the effect of the tip clearance flow on the stage efficiency and stall margin for the tip-limited compressor. Third, a novel analysis approach for tip-critical compressor blade rows is presented by analyzing the axial entropy development within the rotor clearance.

NUMERICAL TOOLS AND STAGE SETUP

The numerical tools for modeling the the compact HPC stage are part of the ANSYS 2019 R1 software suite of the ANSYS, Inc. The geometrical generation of the blade geometries is carried out with the aid of the ANSYS BladeModeler. The spatial discretization of the fluid domains is conducted via the ANSYS meshing tool TurboGrid. The modeling, solving and post-processing of the fluid regime is executed by the ANSYS Inc. RANS/URANS software CFX and CFD-Post. Regarding the design of the bladerows, two different approaches exist, which apply for the present studies. First, full stage calculations considering all relevant blade rows are conducted to gain detailed insight into the stage's aerodynamic phenomena and the blade row interactions. Second, coarse single blade row (SBR) calculations are performed to ensure short turnaround times between different blade design iterations while capturing three-dimensional flow features (e.g. radial re-balancing effects, changes in tip leakage flow). The numerical setup of the fluid domain for the full stage calculation and SBR simulations are listed within Table 1. The mesh element count of the fine meshes is the outcome of a mesh sensitivity study. The end wall resolution of the fine meshes was set to achieve y+ values of $\mathcal{O}(1)$. This ensures a proper resolution of the end wall boundary layers at the hub, shroud and the individual blade rows. For the SBR cases, the mesh count and the resolution of the end-walls were reduced by one order of magnitude. Empirical boundary layer models are used within the regions y+ values of $\mathcal{O}(10)$[1]. This reduction ensures quick turnaround times for the single blade row calculations while giving sufficient insight in the compressor's three-dimensional flow features. The runtime of one SBR operating point is in the order of $1.5 \cdot 10^3$ CPU seconds, which is equivalent to 10 - 20 minutes on a local workstation pc while utilizing of two cores. A consideration of the entire stage leads to a runtime of $1.7 \cdot 10^5$ CPU seconds. Therefore, modern high performance computers are required to simulate the full stage cases within a feasible time frame. By combining the full stage and the SBR simulation approach, a quick design of the compressor could be performed. The inlet of both, the full stage and the SBR cases, are defined by radial distributions of total pressure p_t, total temperature T_t, absolute flow angle α, turbulence kinetic

[1]The $y+ = \mathcal{O}(10)$ is a result from the automated blade mesher TurboGrid when setting the target mesh element count to 10^5. The value is given for the sake of completeness and has no further physical meaning.

Table 2: **Comparison of configurational and geometrical properties of Baseline Compressor and Redesigned Compressor**

Parameter	Baseline Compressor	Redesigned Compressor
R1 Design TPR	1.201	1.239
Design Mass Flow	24.95 kg/s	27.00 kg/s
Rotor Clearance	1.9% span height	3.7% span height
Rotor & Stator Blade Count	48 Rotor & 96 Stator Blades	60 Rotor & 90 Stator Blades
Rotor, Stator Aspect Ratio	Rotor: 0.82, Stator: 1.16	Rotor: 0.71, Stator: 0.89
Rotor, Stator Solidity	Rotor: 1.03, Stator: 1.41	Rotor: 1.49, Stator: 1.71
Stator Configuration	Cantilevered	Shrouded

energy k and turbulence eddy frequency ω. The outlet is defined via a fixed mass flow. Furthermore, a radial static pressure shape is imposed at the outlet. The integral level of the shape adapts automatically in dependence of the assigned outlet mass flow. The different bladerows are connected via mixing planes in the case of the full stage simulations. Across the mixing plane, the flow quantities mix out and are averaged in circumferential direction. Hereby, the circumferentially averaged p_t is kept constant, while the remaining flow quantities adapt to the increase in entropy across the mixing plane.

NUMERICAL HIGH-PRESSURE COMPRESSOR TEST CASE

The compressor design of the considered HPC configuration derives from a preexisting numerical test case of the Chair of Turbomachinery and Flight Propulsion. The preexisting test case consists of three and a half compressor stages and compromises highly loaded compressor stages and moderate rotor tip clearances. The primary goal of the redesign efforts was to establish an even higher loaded compressor stage with large rotor tip clearances. This paper focuses on the redesign of the first stage (rotor 1 and stator 1) of the HPC. The stator trailing edge flow angle distributions were fixed in order to enable an independent redesign of the individual stages. The increase in stage loading, as well as rotor tip clearance, leads to numerous geometrical and configurational modifications for the HPC blade rows. These changes are summarized in Table 2. The increase in rotor 1 relative rotor tip clearance results in a strong destabilization in the casing regions of the compressor. Therefore, a decrease in the aspect ratio of rotor 1 and stator 1 was considered by 13% and 23% respectively. This decrease in aspect ratio leads to an increase of the overall blade solidity in combination with the changes in blade count. The aspect ratio decrease and solidity increase target to enhance the stability of the compressor flow.

Shrouded stators were modeled for the redesigned case. Due to the change in stator configuration, the stator thickness was also modified towards distributions representative for shrouded stators. The stator blade count is set to a multiple of the rotor blade count's fractional to provide the capability for sliding mesh unsteady RANS simulations for follow up investigations. Further changes in compressor design by means of three-dimensional blade features are required to mitigate the detrimental aerodynamic effects caused by the rotor tip clearance flow.

ITERATIVE REDESIGN STRATEGY

The iterative scheme for the redesign of the baseline blading towards a compressor configuration representative for compact HPC rear stages combines two steps:

- Full stage simulations on fine meshes
- Single blade row (SBR) simulations on coarse meshes

The full stage simulations utilize the fine grids for the individual blade rows of the considered stage as well as the stator cavities and aim to capture the three-dimensional flow features within the stage.

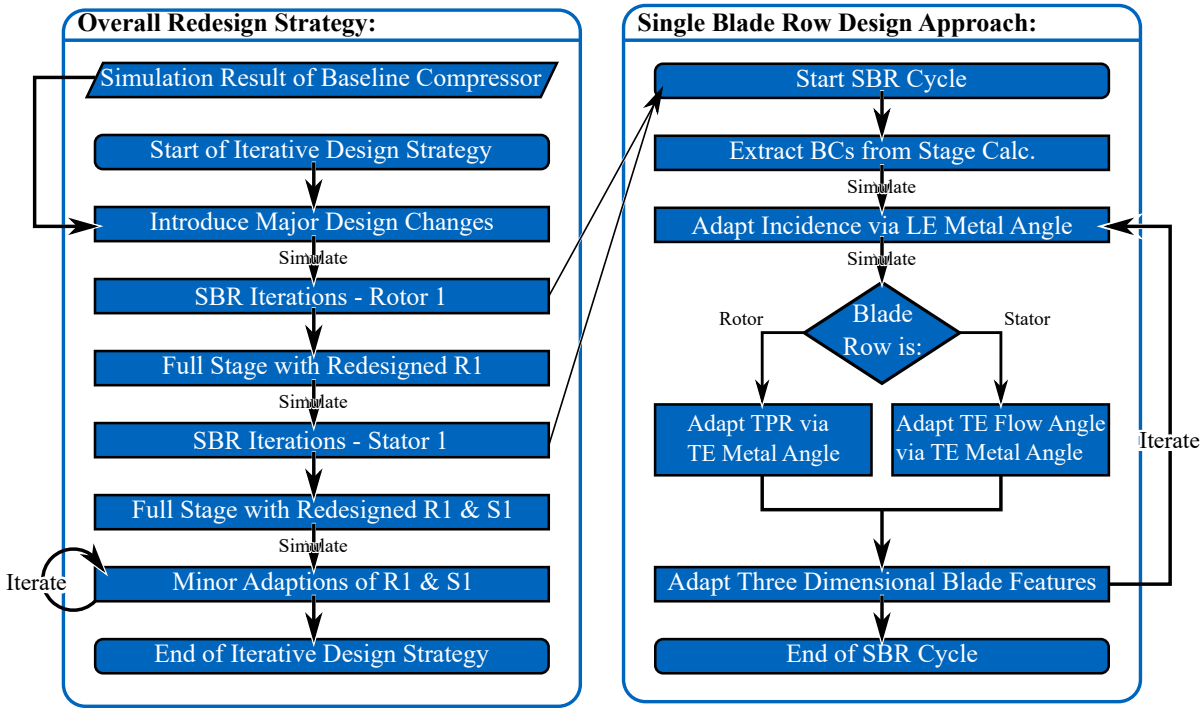

Figure 1: **Redesign strategy for the first high-pressure compressor stage, combining full stage calculations and single blade row simulation cycles**

Furthermore, the interaction of the individual blade rows is captured. The SBR calculations consider only one blade row and the stator cavity if the stator is considered. The boundary conditions (BC) for the full stage calculations are held fixed, while the BCs for the SBR calculations are taken from the inlet, outlet and interfaces of the different domains of the full-stage analyses. By utilizing the SBR approach on coarse meshes, quick turnaround times between the different design iterations could be established. A consideration of the entire stage on coarse meshes would have doubled the simulation time per design iteration. The SBR approach allows furthermore for an independent and systematic design of the different blade rows. The studies associated with the presented design strategy found, that the SBR approach is an effective measure to evaluate the behavior of the individual blades on a delta basis. This way, enhancements in blade row design between the design iterations could be identified. The SBR iterations cover a fully automatized process chain of geometry, mesh and CFD setup generation. After each CFD run, the blade geometry is manipulated manually based on the outcome of the simulation results.

The presented redesign strategy consists of multiple steps (cf. Figure 1). Initially, all significant configurational changes as listed within Table 2 are implemented in the CFD model. The model is then simulated to capture the effects of the changes on the compressor operability and performance. This step is followed by the design of rotor 1 via the SBR iterations on coarse grids. For the SBR iterations of rotor 1, the radial flow quantities at the mixing planes, up- and downstream of rotor 1, are extracted from the initial full stage simulation. Generally, the SBR simulations are then carried out iteratively until:

- A neutral incidence setting ($i = 0$ °) of the blade row at design flow conditions is achieved (adapted LE metal angle) to operate the blades at their efficiency maximum and loss minimum, respectively.
- The target TPR at design flow conditions is achieved if a rotor is considered (adapted TE metal angle).
- The target TE flow angle distribution is achieved if a stator is considered (adapted TE metal angle).

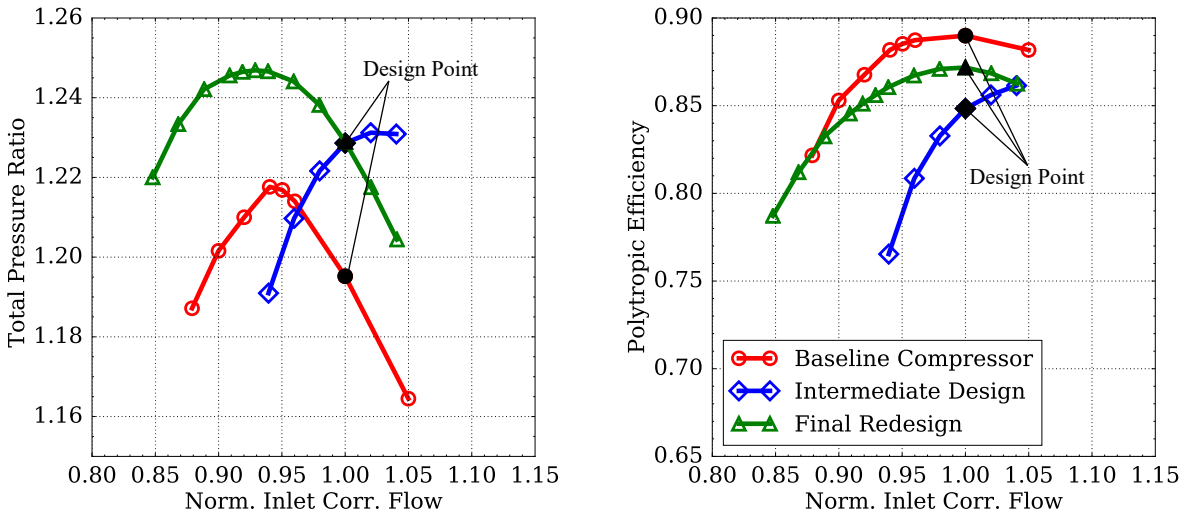

Figure 2: **Stage characteristics of the baseline compressor, intermediate design step and final redesign**

- Sufficient stall margin is acquired and, or no premature blade row stall occurs (adapted TE metal angle, flowpath outline and blade 3D features).

The SBR redesign of rotor 1 is followed by a full stage calculation to capture the effect of the new rotor design on the downstream stator 1. Afterwards, the SBR iterations of stator 1 are performed together with the updated stator 1 inlet conditions. After redesigning rotor 1 and stator 1, the full stage is again simulated, and minor adaptions are performed to assure proper matching of the blade rows. The result of this redesign strategy features blade rows, which are appropriately designed for the new design conditions at a sufficient level of efficiency and stall margin. The compressor, designed with the aid of the presented redesign strategy, is described within the following section.

REDESIGNED BASELINE COMPRESSOR

This section presents the characteristics and performance of the first stage of the redesigned compressor rear stage concept. The concept is representative for highly loaded, compact HPCs as applied in novel aero-engines. The results of the redesign are compared to the baseline compressor and an intermediate design step (cf. Figure 2). The intermediate design step features all configurational changes, as listed in Table 2. Beyond these changes, the rotor turning was increased to meet the TPR at the design mass flow. The operating range of all further presented results is analyzed via the stall margin SM as follows:

$$SM = \left(\frac{\Pi_{t,Peak}}{\Pi_{t,DP}} \cdot \frac{\dot{m}_{IC,DP}}{\dot{m}_{IC,Peak}} - 1 \right) \cdot 100\% \tag{1}$$

The total pressure ratios within Equation 1 consider the stage's outlet and inlet total pressures for the design point (DP) and peak total pressure point[2] (Peak), respectively. The inlet corrected flows $\dot{m}_{IC}$ are taken accordingly for these points. All shown points were generated with the aid of steady state RANS simulations. The convergence criteria of all operating points until the peak pressure of the characteristics were the RMS-residuals of mass and momentum lower than $4 \cdot 10^{-6}$. All further throttled points were in

[2]The peak total pressure point corresponds to the numerical stall point of the compressor configuration. A subsequent check with unsteady RANS simulations lead to similar results for the peak total pressure point as well as the rolled over points. A evaluation of the steady RANS points is therefore feasible.

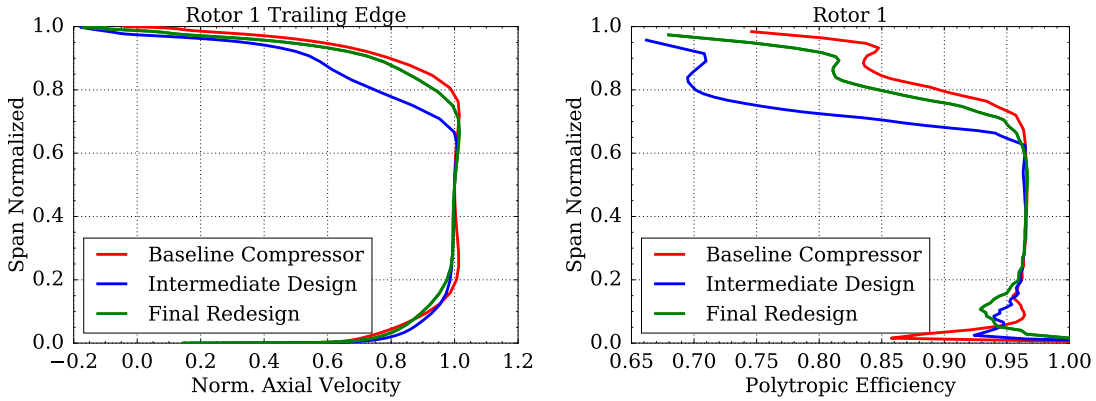

Figure 3: **Span-wise flow distributions: Normalized axial velocity at rotor 1 trailing edge (left) and rotor 1 polytropic efficiency (right) at design flow conditions**

the order of RMS $< 1 \cdot 10^{-4}$. Rolled over points have been checked manually regarding the convergence of the flow field for mass flow and total pressure ratio.

The baseline compressor configuration exhibits a stall margin of 8.3% as well as a maximum of the efficiency in its design mass flow operating point. The characteristics of the intermediate design step show an unstable operation of the compressor stage throughout all considered operation points. This operation substantiates the necessity to enhance the blade design of this compressor configuration. A key aspect for the unstable operation is the occurrence of a strong double leakage flow. This phenomenon could be captured accurately by both, the full stage and the SBR iterations on coarse grids. Deviations of the double leakage axial position between coarse SBR and fine stage calculations were low. The delta was hereby below 2% in streamwise position from LE to TE. By applying the redesign strategy presented in Figure 1, a final redesign could be established. The redesigned compressor stage provides a stall margin of 9.2% as well as an operation of the stage in its efficiency maximum at design flow conditions. The efficiency penalty from baseline compressor to the final redesign is 1.8%. The breakdown of the flow for throttled cases appears within the rotor tip regions for all three compressor designs. The breakdown within the rotor tip region is associated with a growth of low axial momentum regions near the casing of rotor 1 as the compressor is throttled. Furthermore, a strong decrease in the polytropic efficiency distribution occurs near the rotor 1 tip as the flow breaks down. The compressor rotor is the bottleneck of the stage when considering the stage operability. This is due to the large rotor tip clearances. Therefore, the rotor has to be treated with high importance. The stator, however, is of minor importance for the flow stability of the present design. Though, enhancements within the stator regime, e.g. throughout 3D features, helped to reduce the stator total pressure loss at throttled operating points. This goes along with an increase in stage efficiency. Figure 3 (left) shows the span-wise distribution of the normalized axial velocity at the rotor 1 trailing edge for the compressor designs at design flow conditions. The velocities are normalized with the corresponding axial velocities at 50% flow channel height of the respective cases. The baseline case (low rotor 1 tip clearance) and the final redesign (large rotor 1 tip clearance) exhibit a similar radial extend of the tip vortex (large blockage regions with low axial momentum) from the compressor shroud towards the lower span heights. The tip vortex for these cases extends from the tip towards roughly 75% flow channel height. However, the flow of the intermediate design case shows a more significant blockage region extending from the rotor casing to approximately 65% flow channel height. This large region of low momentum fluid limits the compressor operability and leads to a unstable operation of the intermediate design even at design flow conditions. Figure 3 (right) visualizes the span-wise polytropic efficiency distributions of the rotors for the three configurations. The intermediate design provides the lowest efficiency near the rotor casing. The baseline as well as

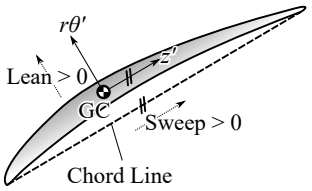

Figure 4: **Parameterization of three dimensional features within airfoil coordinate system ($r\theta'$, z'-system together with airfoil geometrical center (GC)**

Table 3: **Summary of three dimensional blade design features for baseline and redesigned compressor, all quantities are non-dimensionalized with their respective flow channel height or blade chord**

		R1 Baseline					
Span Height	**[% Channel Height]**	100.0	77.1		40.5	22.3	0.0
Sweep	**[% Blade Chord]**	-13.0	-4.5		0.0	0.3	2.4
Lean	**[% Blade Chord]**	4.0	1.5		0.0	0.2	5.5
		S1 Baseline					
Span Height	**[% Channel Height]**	100.0	76.3	67.3	49.4	15.3	0.0
Sweep	**[% Blade Chord]**	3.2	0.1	-0.3	0	-1.4	-0.9
Lean	**[% Blade Chord]**	25.0	15.0	11.5	5.2	1.3	5.2
		R1 Redesign					
Span Height	**[% Channel Height]**	100.0	77.1	58.5	40.5	22.3	0.0
Sweep	**[% Blade Chord]**	0.0	8.0	10.0	12.0	12.0	10.0
Lean	**[% Blade Chord]**	0.0	0.0	0.0	0.0	0.0	0.0
		S1 Redesign					
Span Height	**[% Channel Height]**	100.0	76.3	67.3	49.4	15.3	0.0
Sweep	**[% Blade Chord]**	3.2	0.1	-0.3	-3.0	-9.40	-12.9
Lean	**[% Blade Chord]**	25.0	15.0	11.5	5.2	1.3	5.2

the final redesign of the compressor provide higher efficiency values in the outer flow regions. The presented findings agree with the investigations of Erler et al. (2016). An enhancement in stall margin and efficiency for a critical tip compressor can be mainly achieved by increasing the axial momentum near the rotor tip. The following paragraph summarizes the different design measures used for the final redesign of the compressor. A minor increase in contraction of the outer casing over the rotor tip improved stability of the rotor flow. The contraction increases the axial momentum within the blade's tip regions. Through an adaption of the rotor sweep and bow an additional rise in tip axial momentum could be established. For the presented case all design measures need to target the improvement of the rotor stability in its tip region by increasing the tip axial momentum. The redesign of the stator combines both, sweep and bow. These measures helped to suppress weaknesses within the stator hub regions. A summarizing comparison of the 3D features of the baseline and redesigned compressor is given within table 3. The listed features are oriented in the airfoil coordinate system $r\theta'$,z' (cf. figure 4). The base of this coordinate system is the geometrical center (GC) of each airfoil section. Each quantity given within table 3 describes a manipulation of the corresponding airfoil section within the $r\theta'$,z'-system away from the blade's radial stacking line. The quantities are furthermore non-dimensionalized with the chord-length at the blade's individual span heights. The baseline compressor is designed via five rotor sections and six stator sections. The redesign, however, is defined via six rotor and six stator sections (cf. table 3). This allowed for a detailed design of the flow features across throughout the blade's span.

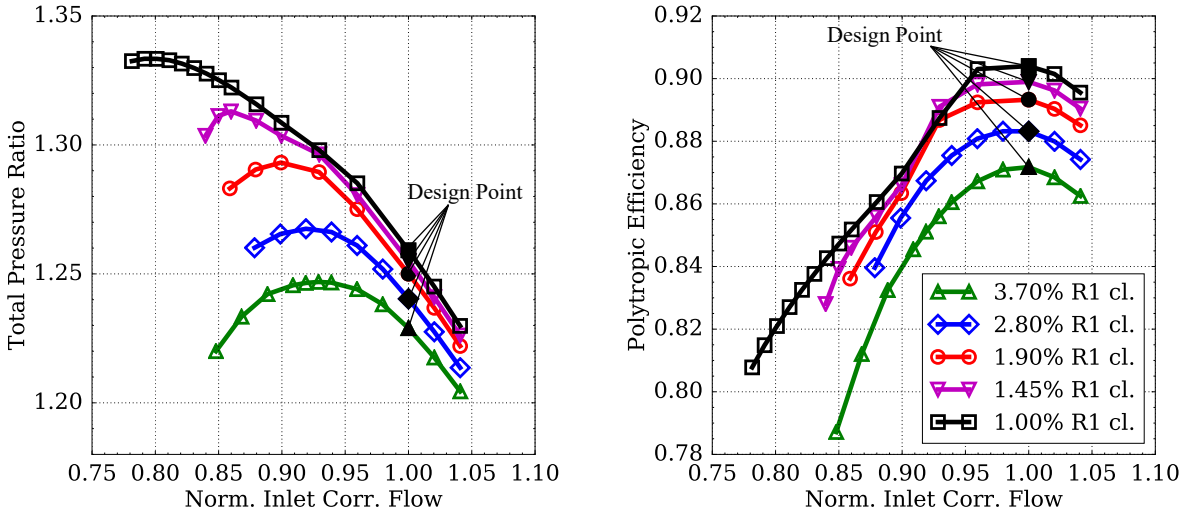

Figure 5: **Stage characteristics of the tip clearance sensitivity study cases**

Table 4: **Increase of stall margin and design point efficiency for lower clearance cases on an absolute delta basis**

Clearance Height	[%]	**2.80**	**1.90**	**1.45**	**1.00**
Stage Stall Margin Delta	[%]	+1.98	+5.81	+12.47	+25.20
Stage DP Efficiency Delta	[%]	+1.15	+2.16	+ 2.73	+ 3.23

Subsequently to the compressor redesign, a rotor tip clearance sensitivity study was performed. A reduction of the rotor tip clearance height enhances the rotor tip flow and axial momentum. The study proves that these enhancements are the main driver for an increase in stage operability and performance for the presented compressor.

SENSITIVITY STUDY - ROTOR TIP CLEARANCE

This section summarizes the findings of the rotor tip clearance sensitivity study. The study was performed with the final redesign case of the compressor stage. Throughout the study, the rotor 1 tip clearance was gradually reduced, while leaving all remaining geometric characteristics of the compressor stage unchanged. The aim of this study is to justify the hypothesis that the enhancement of the rotor tip flow is the main driver for an enhancement of the compressor's operational behavior and performance. The different tested relative tip clearance heights cl are: 3.7% (design clearance of final redesign case), 2.8%, 1.9% (design clearance of baseline compressor case), 1.45% and 1.0% flow channel height. Hereby, the element count and first element offset within the R1 tip clearance is kept constant as the clearance is gradually reduced.

Figure 5 shows the sensitivity of the normalized stage characteristics. With a reduction in relative rotor tip clearance, the operability (stall margin) and performance (efficiency) can be enhanced. This is due to the reduction of the rotor tip vortex and the associated increase in tip axial momentum. Table 4 quantifies the enhancement of stage design point (DP) efficiency and stall margin regarding the final redesign with cl = 3.70%. The increase in stage stall margin as well as the DP efficiency is further visualized in Figure 6. For the presented tip-critical compressor blading, the stall margin increases exponentially as the tip clearance is reduced ($|\Delta cl|$ increase). This can be expressed via a non-linear model as shown by the dashed line in Figure 6 (left). The design point stage efficiency increases linearly

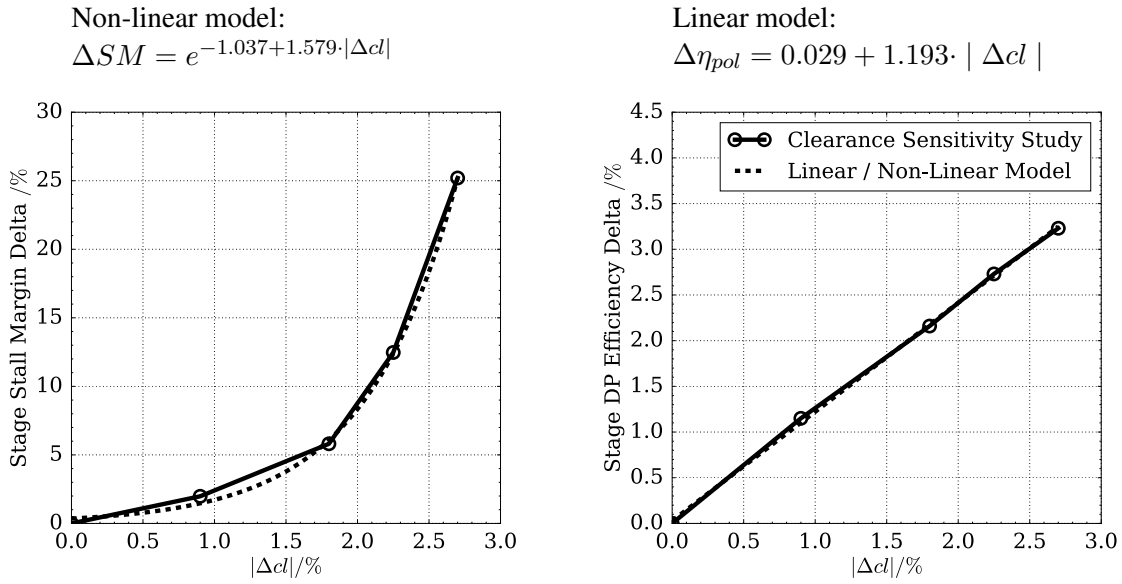

Figure 6: **Development of stage stall margin (left) and design point efficiency (right) throughout rotor tip clearance change relative to design clearance of 3.7%**

for smaller rotor tip clearances. This efficiency increase is expressed by a linear model (cf. Figure 6 right). It is important to note that the dependence of stall margin and efficiency on the decrease in rotor tip clearance only appears for compressor configurations that show a strong rotor tip-critical behavior as in the present design clearance case.

The stall margin of a compressor can only be determined if it is throttled up to its stability limit. Therefore, it is of high interest to estimate the compressor stability already from its flow features at the design condition. A novel approach is presented for analyzing the stability behavior of a rotor tip critical compressor. This approach considers the spike stall criteria of Vo et al. (2008)). The investigations of Vo et al. (2008) focus on the analysis of contour plots to determine the alignment of the loss interface with the leading edge plane. This paper targets a different visualization approach. The presented study investigates the axial development of the circumferentially averaged entropy near the outer casing of the rotor. Figure 7 (left) shows the axial distributions of the circumferentially averaged entropy[3] within the rotor tip clearance region at 98% flow channel height for the redesigned compressor with the relative rotor design clearance of 3.7%. The distributions for the design point (green), peak pressure (blue) and post-stall operating point (red) show a steady increase in entropy level as well as an upstream movement of the entropy peak and gradient as the compressor is throttled. Within the stalled operating condition, the strong positive gradient of the entropy distribution lines up with the axial position of the rotor leading edge near the tip. This phenomenon is equivalent to the first spike stall criterion, as described in Vo et al. (2008). Figure 7 further visualizes the intersection of the rotor tip leakage flow for the post-stall operating point of the redesigned compressor. Besides the alignment of the upstream streamlines with the leading edge plane of the rotor, a significant amount of double tip leakage flow occurs. Furthermore, a part of the tip leakage flow reenters the blade passage from behind the neighboring blade's trailing edge. This phenomenon is also identified by Vo et al. (2008) as the second limiting criterion for the stable operation of the rotor blade row. This trailing edge backflow is also visible for the post-stall case

[3]The averaging is carried out via a averaging function implemented within ANSYS CFD-Post. In a first step, the entropy of entire flow field is circumferentially averaged and weighted with the present mass flow within each control volume. The result is a meridional cross-section of the compressor, which depicts the mean meridional entropy field. In a second step, a interpolation is carried out to extract the entropy values at a fixed span height of 98% flow channel height.

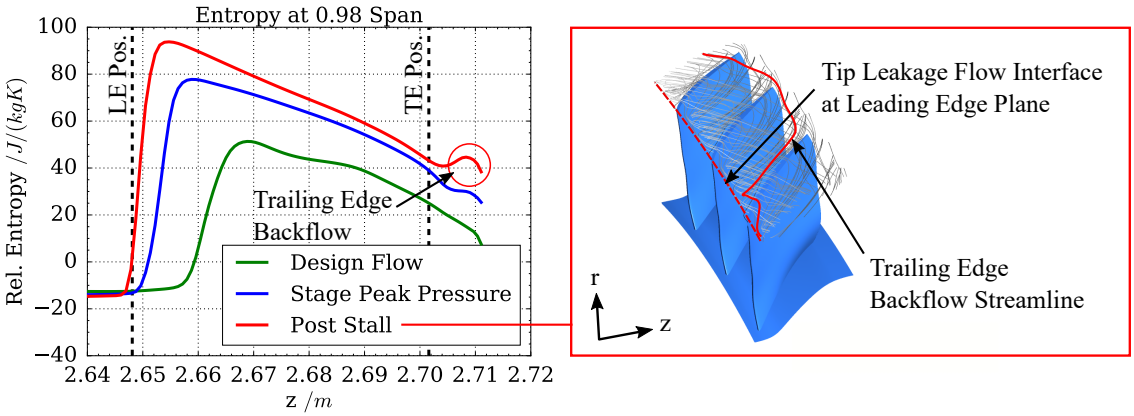

Figure 7: **Circumferentially averaged axial entropy distribution within rotor tip region at 98% flow channel height (left) and post-stall tip clearance streamlines (right)**

in Figure 7 (left) by an increase of the entropy behind the axial rotor trailing edge position. It appears that the stability of a tip-critical rotor is reflected by the axial distance of the entropy development within the tip leakage flow region. Figure 8 shows the axial distance between the entropy peaks of the axial entropy distributions (cf. Figure 7, left) and the rotor leading edge for all available operating points of the tip clearance sensitivity study. The axial distance can be interpreted as a measure of the stability of the rotor. While larger distance values are a sign of stable operation of the rotor blade row, smaller values indicate the proximity of stall initiation. Within design flow conditions (normalized inlet corrected flow = 1.0) the distance tends to increase as the rotor clearance is decreasing. A increase of the axial distance is hinting towards stabilization and strengthening of the flow within the rotor tip region. The distance between entropy maximum and rotor leading edge generally decreases, for all clearance heights as the compressor is throttled. In the case of the 3.70% rotor clearance, the entropy distance decreases monotonously for all operating points. For the remaining clearance heights, a flattening of the curves occurs. As the entropy distance is interpreted as a measure of rotor tip flow stability, the flattening of the individual curves for higher degrees of throttling indicates an stabilization of the rotor tip flow. This effect can be explained by the appearance of flow separations within the downstream stator 1 hub regions. Due to these flow separations, a radial redistribution of the flow occurs. The upstream effect of this radial redistribution increases the axial momentum in the rotor 1 tip regions and therefore stabilizes the rotor tip flow. This stabilizing effect amplifies towards lower rotor clearance heights and is most pronounced for 1.00% rotor 1 clearance height. For this case, initial instabilities of stator 1 appear at 93% normalized inlet corrected flow. From this operating point on, a significant flattening of the entropy distance distribution is notable as the stator 1 hub separations enlarge. These separations enhance the axial momentum within the upstream rotor tip regions even though the compressor loading increases monotonously. The result is a strengthening of the rotor tip region. At 80% normalized inlet corrected flow, the stage characteristics show the peak total pressure ratio of the 1.00% rotor tip clearance case (cf. Figure 5 (left)). For even more throttled operating points, the total pressure characteristic rolls over, and unstable operation of the rotor and stage is observed. It appears that the entropy distance distribution drops down to low values for these rolled over points (cf. Figure 8). This indicates a rapid movement of the entropy maximum towards the rotor leading edge. It can also be seen as the initiation of a stall within the rotor. The analysis of the circumferentially averaged axial entropy distribution within the rotor tip region is useful way to analyze the stability behavior of a whole compressor stage with a tip-critical rotor.

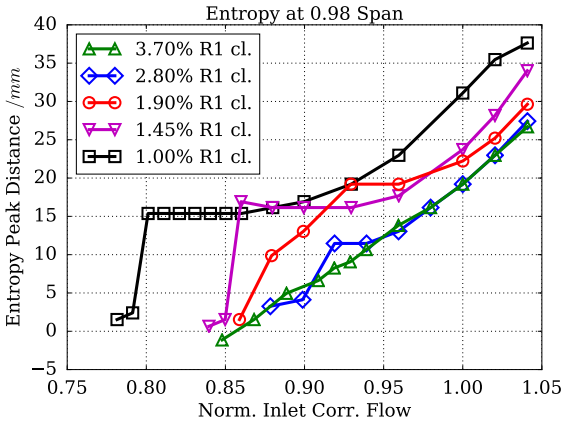

Figure 8: **Axial distance between leading edge and entropy maximum of axial entropy distribution within rotor tip region at 98% flow channel height over the normalized corrected mass flow**

CONCLUSIONS

The analysis of this paper is divided into three parts: The redesign scheme and results of an existing compressor stage towards a configuration representative for highly loaded, compact HPC rear stages, a tip clearance sensitivity study of the redesigned compressor stage and a novel way to analyze the stability of rotor tip-critical compressors. The presented redesign scheme solely utilizes three-dimensional RANS simulations on different mesh resolutions. With the aid of the described design scheme, a novel HPC design compromising high blade loadings and large relative rotor tip clearances could be established successfully. It shows that this design scheme is feasible for a quick redesign of existing compressor configurations. The stage stall margin of the redesign could be increased by 0.9%. An efficiency decrease of 1.8% resulted. This efficiency penalty could not be prevented due to the significant increase in tip clearance height by approximately 100%. It appeared that the major limiting factor of the stage stability is the weak tip clearance flow of the rotor due to the large relative tip clearance height. Therefore, the majority of the design efforts need to target towards stabilization of the rotor tip flow. This can be achieved by an increase in rotor tip axial momentum. The utilization of the axial entropy development is a feasible way to analyze the stability behavior of a rotor tip-critical compressor stage. This entropy analysis could be leveraged to be used as a stall prediction method within modern compressor test benches, which utilize high-frequency entropy measurements by determining the development of the total pressure as well as temperature. Such measuring techniques were investigated in e.g. Mansour et al. (2008a), Mansour et al. (2008b) and Mansour et al. (2012).

ACKNOWLEDGMENTS

This project has received funding from the Clean Sky 2 Joint Undertaking (JU) under grant agreement No 821435. The JU receives support from the European Union's Horizon 2020 research and innovation programme and the Clean Sky 2 JU members other than the Union.

REFERENCES

Copenhaver, W. W., Mayhew, E. R., Hah, C., and Wadia, A. R. (1996). The effect of tip clearance on a swept transonic compressor rotor. *Journal of Turbomachinery*, 118(2):230–239.

Denton, J. D. (2017). Multall—an open source, computational fluid dynamics based, turbomachinery design system. *Journal of Turbomachinery*, 139(12):125.

Erler, E., Vo, H. D., and Yu, H. (2016). Desensitization of axial compressor performance and stability to tip clearance size. *Journal of Turbomachinery*, 138(3):491413.

Hah, C. (2017). Effects of double-leakage tip clearance flow on the performance of a compressor stage with a large rotor tip gap. *Journal of Turbomachinery*, 139(6):15.

Hah, C., Hathaway, M., and Katz, J. (06162014). Investigation of unsteady flow field in a low-speed one and a half stage axial compressor: Effects of tip gap size on the tip clearance flow structure at near stall operation. In *Volume 2D: Turbomachinery*. American Society of Mechanical Engineers.

Hah, C., Hathaway, M., Katz, J., and Tan, D. (07262015). Investigation of unsteady tip clearance flow in a low-speed one and half stage axial compressor with les and piv. In *Volume 1: Symposia*. American Society of Mechanical Engineers.

Inoue, M., Kuroumaru, M., Yoshida, S., Minami, T., Yamada, K., and Furukawa, M. (06142004). Effect of tip clearance on stall evolution process in a low-speed axial compressor stage. In *Volume 5: Turbo Expo 2004, Parts A and B*, pages 385–394. ASMEDC.

International Air Transport Association (2016). Iata forecasts passenger demand to double over 20 years.

Mansour, M., Chokani, N., Kalfas, A. I., and Abhari, R. S. (2008a). Time-resolved entropy measurements using a fast response entropy probe. *Measurement Science and Technology*, 19(11):115401.

Mansour, M., Chokani, N., Kalfas, A. I., and Abhari, R. S. (2008b). Unsteady entropy measurements in a high-speed radial compressor. *Journal of Turbomachinery*, 130(2):521.

Mansour, M., Chokani, N., Kalfas, A. I., and Abhari, R. S. (2012). Impact of time-resolved entropy measurement on a one-and-one-half-stage axial turbine performance. *Journal of Turbomachinery*, 134(2):79.

Vo, H. D., Tan, C. S., and Greitzer, E. M. (2008). Criteria for spike initiated rotating stall. *Journal of Turbomachinery*, 130(1):68.

Yamada, K., Kikuta, H., Furukawa, M., Gunjishima, S., and Hara, Y. (06032013). Effects of tip clearance on the stall inception process in an axial compressor rotor. In *Volume 6C: Turbomachinery*. American Society of Mechanical Engineers.